

## Peroxide bond strength of antimalarial drugs containing an endoperoxide cycle. Relation with biological activity†‡

Israel Fernández\*<sup>a</sup> and Anne Robert\*<sup>b</sup>

Received 17th January 2011, Accepted 17th February 2011

DOI: 10.1039/c1ob05088e

Several endoperoxide compounds are very efficient antimalarial analogues of the natural drug artemisinin. Quantum chemical calculations have been used to correlate the computed free energies of the O–O bond with respect to the total number of oxygen atoms contained in the cycle, and with the size/strain of the cycle (5- or 6-membered cycles). The gas-phase homolysis of the O–O bond has been studied for five- and six-membered oxygenated cycles which are models of the “real” drugs. Our results indicate that, in 6-membered cycles, the stability order is the following: 1,2-dioxane > 1,2,4-trioxane > 1,2,4,5-tetraoxane. In cycles containing 3 oxygen atoms, the 5-membered cycle 1,2,4-trioxolane was found much less stable than its 6-membered counterpart 1,2,4-trioxane. This feature indicates the possible role of the cycle strain for the O–O bond stability, and may also explain the high antimalarial activity of some trioxolane derivatives. Similar trends in the O–O bond strength have been found for the real antimalarial drugs. However, the O–O bond stability is not in itself a decisive argument to anticipate the antimalarial activity of drugs.

### Introduction

Artemisinin, an antimalarial drug extracted from the Chinese herb *Artemisia annua*, is highly active against both chloroquine-sensitive and chloroquine-resistant strains of *Plasmodium falciparum* (Pf), the most virulent species of the malaria parasite,<sup>1–3</sup> and Artemisinin Combination Therapies (ACTs) are now recommended (see Scheme 1 for the structure of artemisinin).<sup>4,5</sup>

Artemisinin is one of the few examples of natural sesquiterpene containing a 1,2,4-trioxane as a pharmacophore. The removal of one O-atom of the peroxide bridge is associated with complete loss of the antimalarial activity of the drug,<sup>1,6,7</sup> artemisinin *in vitro* activity being higher by three orders of magnitude as that of the 1-deoxy derivative (IC<sub>50</sub> value of artemisinin on the chloroquine-resistant Pf strain FcM29-Cameroon is 11 nM, compared to 5000–10000 for 1-deoxyartemisinin, Scheme 1).<sup>8</sup> Replacement of the non peroxidic oxygen atom of the trioxane ring of artemisinin, O13, by a methylene unit has also been carried out.<sup>9a</sup> The resulting 13-carbaartemisinin (**7**, Scheme 1), which had no longer trioxane ring but a 1,2-dioxane, displayed a less potent antimalarial activity

than artemisinin. However, it was still significantly active, with an IC<sub>50</sub> value of 45 nM on the W2-Indochina strain (25 times higher as that of artemisinin: 1.7 nM). Many semisynthetic derivatives modified at C10 were reported as active antimalarial drugs, among them are the 10-deoxoartemisinin,<sup>9b</sup> artemisone,<sup>9c</sup> and the clinically used artemether and artesunate. Many research groups have prepared fully synthetic peroxide-containing analogues. Some of these compounds are highly potent antimalarials. Among them are the trioxaquinones containing a 1,2,4-trioxane as artemisinin does,<sup>10–12</sup> 1,2,4-trioxolanes such as OZ277,<sup>13–15</sup> and 1,2,4,5-tetraoxanes (Fig. 1).<sup>16–18</sup>

Due to the low energy of their O–O σ\* LUMO orbital, organic peroxides are usually unstable and explosive, specially when heated, and the control of their reactivity is difficult.<sup>19,20</sup> Unexpectedly, artemisinin does not decompose at its melting temperature (156–157 °C); it is also stable in solution heated up to 150 °C. The thermal rearrangement and decomposition products of artemisinin at 190 °C have been reported.<sup>21</sup> High melting point without decomposition have also been reported for OZ277 (160–162 °C), 13-carbaartemisinin (160–162 °C),<sup>9a</sup> and 1,2,4,5-tetraoxane RKA182 (179–181 °C for the ditosylate salt).<sup>18b</sup> Other synthetic trioxanes can be heated up to 180–200 °C.<sup>22</sup>

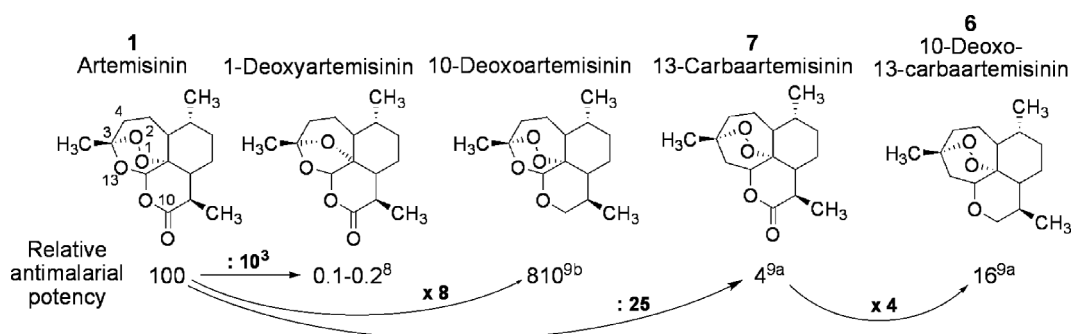
After more than two decades of intensive studies, the mechanism of action of artemisinin is still controversial. However, alkylating species generated by ferrous iron-mediated homolytic cleavage of the endoperoxide function of artemisinin, in particular the alkyl radical centered at C4 of artemisinin (or related 1,2,4-trioxanes), were early proposed to be important (see Scheme 1 for numbering of atoms of artemisinin).<sup>23</sup> We have reported that iron(II)-heme

<sup>a</sup>Departamento de Química Orgánica, Facultad de Química, Universidad Complutense, 28040, Madrid, Spain. E-mail: israel@quim.ucm.es; Fax: (+34)913944310

<sup>b</sup>Laboratoire de Chimie de Coordination du CNRS, 205 route de Narbonne, 31077, Toulouse Cedex 4, France. E-mail: Anne.Robert@lcc-toulouse.fr; Fax: (+33)561553003

† Electronic supplementary information (ESI) available: Cartesian coordinates and total energies of all drugs discussed in the text. See DOI: 10.1039/c1ob05088e

‡ This article is dedicated to Dr Bernard Meunier



**Scheme 1** Structures of artemisinin and 13-carbaartemisinin derivatives. Relative antimalarial activities =  $IC_{50}$  of analog/ $IC_{50}$  of artemisinin, on *P. falciparum*. Comparison of artemisinin **1** and 1-deoxyartemisinin in reference 8 (FcM29-Cameroon strain); comparison of **1**, **6**, and **7** in reference 9a (W2-Indochina strain); comparison of **1** and 10-deoxyartemisinin in reference 9b (W2-Indochina strain).

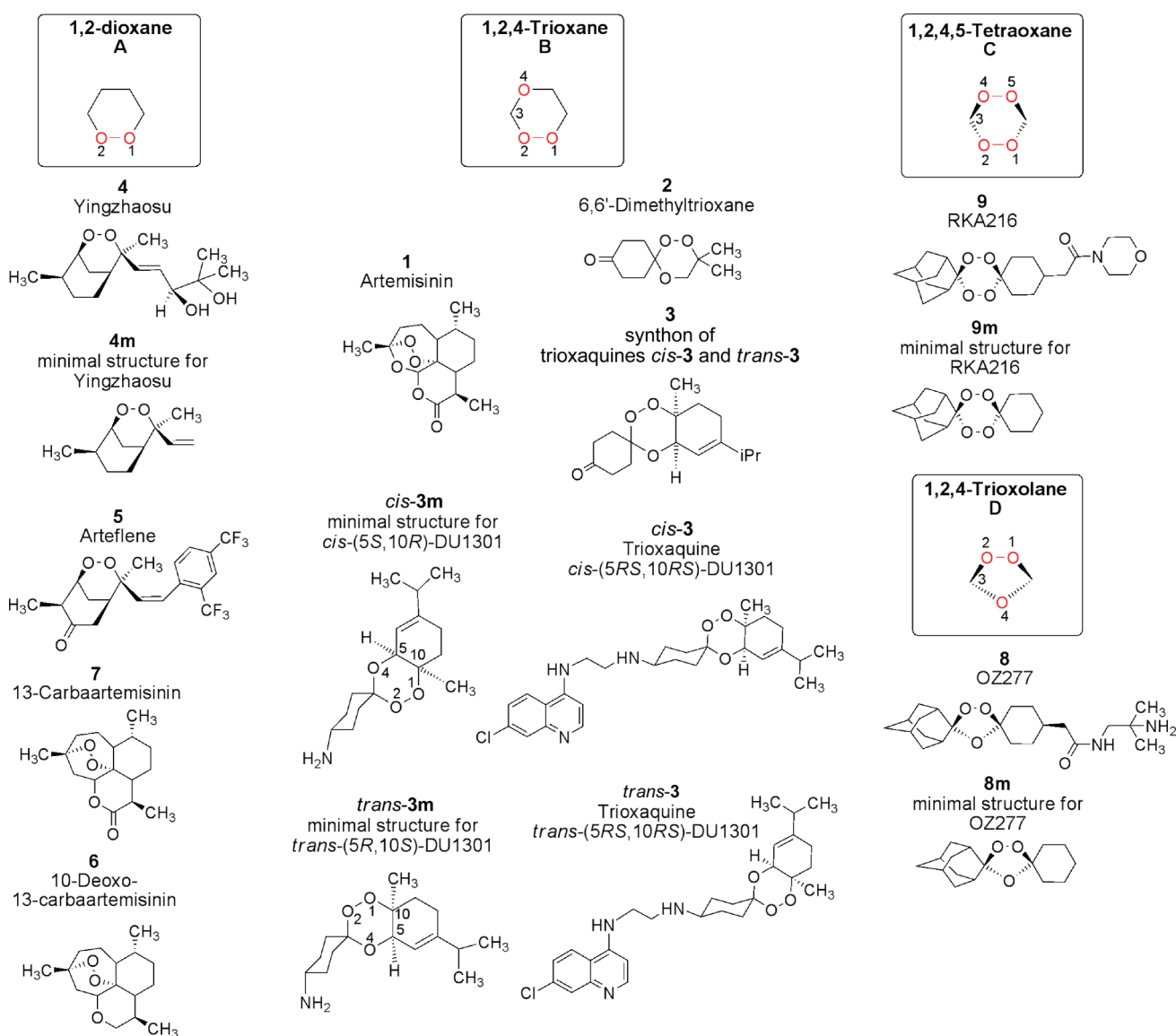


**Fig. 1** Structures of the antimalarial drugs and analogs computed at the B3LYP/6-31+G(d) level: 1,2-dioxanes (**A**), 1,2,4-trioxanes (**B**), 1,2,4,5-tetraoxane (**C**), and trioxolane (**D**).

incubated with artemisinin was readily converted in high yield to heme-artemisinin covalent adducts resulting from alkylation of the four *meso* positions of the porphyrin ligand by the C4-alkyl radical derived from artemisinin.<sup>24–26</sup> The reductive cleavage of artemisinin is initiated by an electron transfer from the low-valent iron(II)-heme to the antibonding  $\sigma^*$  orbital of the peroxide bond. This reductive activation generates a short lived alkoxy radical which quickly rearranges, *via*  $\beta$ -fragmentation, to a C4-centered primary radical thermodynamically facilitated by the concomitant formation of an ester functionality.<sup>26</sup>

The alkylating ability of artemisinin is not limited to this natural compound. A number of active semi-synthetic derivatives modified at position C10 (either with  $\alpha$  or  $\beta$  configuration) were found to react in the same way.<sup>27–30</sup> Synthetic trioxanes or trioxolanes were also able to alkylate heme or a synthetic heme model, and their alkylation ability correlates well with their antimalarial efficacy.<sup>31–34</sup> Supporting this hypothesis, the heme-drug adducts were detected in the spleen and urine of *P. vinckei* infected mice, orally treated with artemisinin, or trioxaquinines.<sup>34–36</sup> So, the contribution of this process to parasite death is probable.

To our knowledge, the relative stability of the peroxide bond contained in different hydrocarbon cycles has never been reported. So, we decided to correlate the computed free energies of the O–O bond with respect to the total number of oxygen atoms contained in the cycle, and with the size/strain of the cycle (5- or 6-membered cycles). In the field of antimalarial drugs, relative stability of different cycles containing a peroxide bond is important: the homolysis of the O–O bond is required for biological activity. However, the greatest possible thermal stability of these drugs is obviously requested for both a convenient synthesis process and an easy storage in tropical countries. In addition, the tendency of the different endoperoxides to reductive activation by iron(II) was also computed. In this study, our objective was to determine whether the O–O bond stability/reactivity of the studied drugs can be significantly correlated to their *in vitro* antiplasmodial activity.

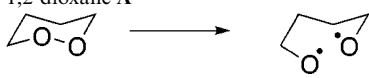
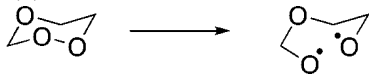
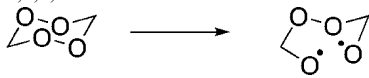
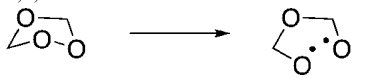
## Results and Discussion

### Homolysis of peroxide bond contained in “naked” 5- and 6-membered cycles

First, we computed the energy associated with the homolysis of the peroxide bond for the simplest 5- and 6-membered cyclic endoperoxides, which leads to the corresponding diradical species. We have explored the formation of diradicals either as triplet or open-shell singlet species. The computed gas-phase total reaction energy values ( $\Delta E$ , zero point energy included) and  $\Delta G_{298}$  free energies of the homolysis of the O–O bond are gathered in Table 1 for 1,2-dioxane **A**, 1,2,4-trioxane **B**, 1,2,4,5-tetraoxane **C** and trioxolane **D** “naked” cycles, *i.e.* without taking substituents into account. In each case, the triplet or open-shell singlet ground state of the produced diradical give rise to two energy values,  $\Delta E(\text{T-S})$  and  $\Delta E(\text{OS-S})$ , respectively. First set of values has been computed at the MP2/6-311 ++ G\*\* level (Table 1, plain values). In the case of the 1,2-dioxane, the triplet state of the product is slightly favored with respect to the singlet state [ $\Delta E = 40.8$  and  $39.0$  kcal mol<sup>-1</sup> for (T-S) and (OS-S), respectively]. For the three other cycles, there is no significant difference of energy between the triplet and open-shell singlet ground states ( $\Delta \leq 0.5$  kcal mol<sup>-1</sup>). So, the energy values obtained by the MP2 method exhibit the same trend for the two possible electronic structures of the product.

Interestingly, for the 6-membered rings, the stability of the peroxide bond follows the order 1,2-dioxane > 1,2,4-trioxane > 1,2,4,5-tetraoxane, with  $\Delta E(\text{T-S})$  values = 40.8, 37.7, and 33.3 kcal mol<sup>-1</sup>, respectively. As expected, the more oxygen atoms in the cycle, the weaker O–O bond, due to a lower electron density in its  $\sigma$ -bonding molecular orbital. This is indeed explained using the second order perturbation theory (SOPT) of the natural bond orbital (NBO) method, which shows a clear two-electron delocalization from the  $\sigma$ -O1–O2 molecular orbital to the  $\sigma^*$  molecular orbital of the adjacent C3–O4 bond of the 1,2,4-trioxane (associated second order energy of  $-0.57$  kcal mol<sup>-1</sup>).

**Table 1** Gas phase total energies plus ZPVE values of the O–O bond in several oxygenated 5- or 6-membered rings. Plain values are computed at the MP2/6-311 ++ G\*\* level, values in italics computed at the B3LYP/6-311 ++ G\*\* level.  $\Delta G_{298}$  free energies are given in parenthesis

Reaction	O–O bond order	$\Delta E(\text{T-S})^a$ kcal mol <sup>-1</sup>	$\Delta E(\text{OS-S})^b$ kcal mol <sup>-1</sup>
1,2-dioxane <b>A</b> 	0.977 (0.963)	+ 40.8 (+ 38.7) + 24.9 (+ 21.9)	+ 39.0 (+ 37.0) + 22.8 (+ 20.7)
1,2,4-trioxane <b>B</b> 	0.974 (0.960)	+ 37.7 (+ 35.4) + 22.0 (+ 19.3)	+ 37.2 (+ 35.2) + 20.5 (+ 18.3)
1,2,4,5-tetraoxane <b>C</b> 	0.974 (0.962)	+ 33.3 (+ 30.8) + 17.2 (+ 14.4)	+ 33.3 (+ 31.5) + 17.8 (+ 15.1)
1,2,4-trioxolane <b>D</b> 	0.971 (0.956)	+ 29.3 (+ 27.7) + 11.9 (+ 10.1)	+ 29.2 (+ 28.2) + 11.8 (+ 10.7)

<sup>a</sup> Triplet minus ground state energies. <sup>b</sup> Open-shell singlet minus ground state energies.

This interaction is not possible in the parent 1,2-dioxane and as a consequence the O–O bond is weaker in 1,2,4-trioxane than in 1,2-dioxane. This is nicely reflected in the computed shorter O1–O2 bond length of naked 1,2-dioxane **A** (1.456 Å) compared to trioxane analogue **B** (1.461 Å). A similar two-electron delocalization was also found in 1,2,4,5-tetraoxane (associated second order energy of  $-0.74$  kcal mol $^{-1}$ ) justifying the highest lability of its O–O bond (Fig. 2).

As readily seen in Table 1, the trend of stability found when one considers the formed diradical as an open-shell singlet is the same than considering triplets. Thus, 1,2-dioxane exhibits a significantly higher stability (40.8 kcal mol $^{-1}$  for its triplet state) with respect to the 1,2,4,5-tetraoxane (33.3 kcal mol $^{-1}$ ), the 1,2,4-trioxane having an intermediate computed stability (37.7 kcal mol $^{-1}$ ). The 5-membered trioxolane was found the least stable [ $\Delta E(\text{T-S}) = 29.3$  kcal mol $^{-1}$ , compared to 37.7 kcal mol $^{-1}$  for 1,2,4-trioxane, its 6-membered counterpart], indicating also that the cycle strain is probably a major contributor.

We also computed the same systems within the density functional theory (DFT) framework using the hybrid B3LYP functional. The obtained gas-phase energy values follows the same order of decreasing stability: 1,2-dioxane (24.9 kcal mol $^{-1}$  for the triplet state) > 1,2,4-trioxane (22.0 kcal mol $^{-1}$ ) > 1,2,4,5-tetraoxane (17.2 kcal mol $^{-1}$ ) > trioxolane (11.9 kcal mol $^{-1}$ ). So, the two methods used provided fully consistent results which indicates that the B3LYP method can be used to gain insight into the stability of the peroxide bond for the more computer-demanding structures such as the real antimalarial drugs (see below).

The NBO-Wiberg bond order of the O–O bond was not found significantly different for the four structures ( $0.960 \pm 0.003$  when computed using B3LYP). This is in agreement with the quite tiny difference found for the O–O bond lengths (see above). This feature may be indicative of the importance of steric factor, which is expected in polycyclic and spiro compounds.

### Reductive activation of naked peroxides by iron(II)

As stated above, the reductive cleavage of artemisinin is initiated by an electron transfer from the low-valent iron(II)-heme to the antibonding  $\sigma^*$  LUMO orbital of the peroxide bond which generates a short lived alkoxy radical.<sup>26</sup> Thus, we decided to

compute this reductive activation of the peroxide bond to gain more insight into the antimalarial activity of the studied systems. To this end, we selected the naked endoperoxides **A–D** considered above (Fig. 1) in their reaction with a model of iron(II)-heme having hydrogen atoms in place of the  $\beta$ -pyrrolic substituent. This reaction, leading to the iron(III)-heme–alkoxy radicals, is depicted in Scheme 2.

As our starting Fe<sup>II</sup>-heme model complex resembles to the Fe<sup>II</sup>-heme in deoxyhemoglobin (or deoxymyoglobin), the high spin electronic configuration was chosen for this species.<sup>37</sup> In fact, our calculations (UB3LYP/def2-SVP level) clearly indicate that the low spin complex of the iron(II)-heme model is 32.5 kcal mol $^{-1}$  higher in energy than its high-spin counterpart. Similarly, the high-spin Fe<sup>III</sup>-product formed after the reductive cleavage of 1,2-dioxane is 11.9 kcal mol $^{-1}$  more stable than its low-spin analogue (only hexacoordination with two strong field axial ligands, such as CN $^-$  or imidazole are known to stabilize low spin iron(III) porphyrins). So, all the energy values of reductive cleavage reactions studied herein have been computed using high-spin heme derivative. For comparison, the reactions using low-spin species were also computed. All data are gathered in Table 2.

The reductive cleavage reaction leads to the formation of products whose unpaired electrons are mainly located in the iron and in the free oxygen atoms (see Fig. 3). For instance, the computed spin densities for the corresponding Fe<sup>III</sup>-complex formed from 1,2-dioxane are 4.16e and 0.88e for the iron ion and alkoxy radical, respectively [Fig. 3 (A)]. Similar values of the computed spin density were found for 1,2,4-trioxane, tetraoxane, and trioxolane (electron densities being in the ranges 4.16–4.18e on iron and 0.79–0.88e on alkoxy radical). For 1,2,4-trioxane, we considered both the coordination of iron onto O1 or O2 [Fig. 3 (B1) and (B2), respectively]. The formation of the **B1** intermediate is indeed the main experimental pathway for activation of artemisinin *in vitro* and *in vivo*,<sup>38</sup> but importance of intermediate **B2** was also suggested.<sup>23</sup> For the other “naked” endoperoxides (namely, trioxolane and tetraoxane), due to symmetry of the structures, coordination of iron onto O1 or O2 leads to the same alkoxy radicals. Furthermore, the pentacoordinated iron atom of the product does not lie in the mean plane of the porphyrin ring, but is located *ca.* 0.6 Å above the mean porphyrin plane (Fig. 3).

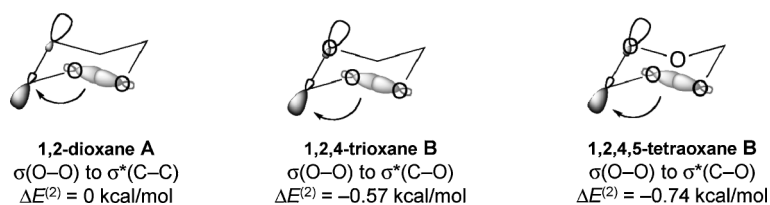
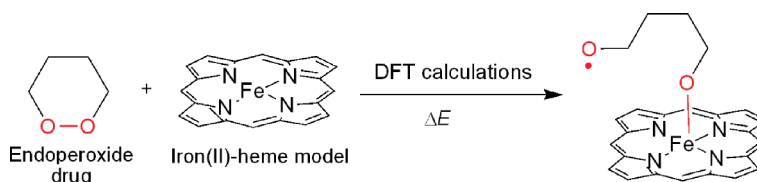
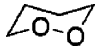
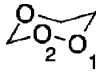
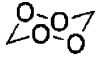
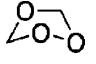


Fig. 2 Two-electron delocalizations (and associated second order perturbation energies) of 6-membered cyclic endoperoxides.



Scheme 2 Reductive activation of endoperoxides by iron(II)-heme.

**Table 2** Gas-phase energies (in kcal mol<sup>-1</sup>) of the iron(II)-heme model (high-spin or low-spin) mediated reductive cleavage of the O–O bond in several oxygenated 5- or 6-membered rings. All values have computed at the B3LYP/def2-SVP level

Endoperoxide drug	$\Delta E$ [high spin] <sup>a</sup> ( $\Delta G_{298}$ ), kcal mol <sup>-1</sup>	$\Delta E$ [low spin] <sup>a</sup> ( $\Delta G_{298}$ ), kcal mol <sup>-1</sup>
	-13.7	-34.3
	(-4.0)	(-24.0)
Fe coordinated on O1	-18.6 (-9.2)	-36.1 (-26.3)
Fe coordinated on O2	(-13.9) -22.8	-41.7
	(-12.8) -26.1	(-32.8) -54.9
	(-16.0)	(-45.3)

<sup>a</sup> Plain values indicate the computed total energies (zero point vibrational energy included). Free energies ( $\Delta G_{298}$ ) are given in parenthesis.

The gas-phase total end free energies for the reductive cleavage of the considered cyclic peroxides are compiled in Table 2 and Scheme 3. As expected, all the reactions are exothermic due to formation of the new O–Fe bond. The computed  $\Delta E$  and  $\Delta G_{298}$  energies follow essentially the same trend: the order of exothermicity is 1,2-dioxane ( $\Delta G_{298} = -4.0$ ) > 1,2,4-trioxane ( $-9.2$ ) > 1,2,4,5-tetraoxane ( $-12.8$ ) > trioxolane ( $-16.0$  kcal mol<sup>-1</sup>). The exothermicity of the reactions is directly related to the strength of the peroxide bond, *i.e.* a weaker O–O bond leads to a more exothermic transformation. Strikingly, the computed trend is exactly the same than that found for the non-metal assisted cleavage of the O–O bond (see above). Therefore, this result provides further support to the stability order computed for the gas-phase breaking of the peroxide bond for the considered antimalarial drugs.

For the case of 1,2,4-trioxane, we also considered the alternative cleavage of the O–O bond due to complexation of O<sub>2</sub> on the iron atom. The computed numbers indicate that the product formed in this process is 4.7 kcal mol<sup>-1</sup> higher in energy than that where the O1 is coordinated to iron. This feature is consistent with the experimental reactivity of heme in the presence of artemisinin and confirms that the preferred coordination of iron(II)-heme on the O1 of artemisinin is not due to steric hindrance factors and/or electronic contribution of the trioxane ring substituents, but also to intrinsic reactivity of its peroxide bond.

### Homolysis of peroxide bond contained in antimalarial drugs

Recent articles report the molecular dynamics and quantum chemistry calculations of artemisinin O–O bond homolysis, either in the absence<sup>39</sup> or in the presence<sup>40</sup> of iron(II) ions, leading to radical structures which may be deleterious for the parasite. In the present study, the energy of the homolysis of the peroxide bond was then computed using B3LYP method for several

antimalarial drugs and related compounds depicted in Fig. 1. For computational reasons, the side chains of some drugs were omitted and “minimal structures” retaining the endoperoxide cycle were considered. The first series is based on a 1,2-dioxane cycle, like **A**. The natural yinghaosu **4**<sup>41</sup> and its synthetic mimic arteflene **5**,<sup>42</sup> which has been under clinical studies in the 1990 s, belong to this series, as well as the 13-carbaartemisinin **7** and 10-deoxy-13-carbaartemisinin **6**. The entire structures of drugs **5**, **6**, and **7** were computed, whereas the minimal structure of yingzhaosu **4m** was retained. The lead compound artemisinin **1** and the trioxanes **2**, *cis*-**3m** and *trans*-**3m**, which are fragments of the dual quinoline-trioxane drugs, trioxaquinones PA1103 and DU1301, respectively, belong to the series based on the 1,2,4-trioxane **B**. The entire structures of **1** and **2** were computed. Trioxaquinones *cis*-**3** and *trans*-**3** being racemic compounds, the minimal structure of a single stereoisomer of each was computed in the present study, namely the trioxanes *cis*-**3m** and *trans*-**3m**. The tetraoxane **9m** and trioxolane **8m** were computed as minimal structures of the tetraoxane RKA216, **9** (series **C**) and the trioxolane OZ277, **8** (series **D**), respectively.

First, the geometry of all structures was optimized at the B3LYP/6-31+G\* level, starting from the X-ray diffraction structures when they were known.<sup>43</sup> The optimized geometries are reported in Fig. 4. The computed bond lengths and angles are very similar to the available experimental data. In particular, the computed O–O bond lengths (in the range 1.458–1.467 Å = 1.463 ± 0.005) for all species concur quite well with the experiment (O–O bond length in the range 1.432–1.480 Å = 1.456 ± 0.024). This supports the double- $\xi$  quality basis set B3LYP/6-31+G(d) level, which was chosen for reducing the computational costs of these medium-size systems.

Table 3 gathers the change in energy associated to the gas-phase homolysis of the O–O bond in the antimalarial drugs leading to the corresponding diradical as triplets. As we consider the breaking of cyclic molecules, the entropic contribution should be important. In fact, the significant role of the cycle strain was reported above (Tables 1 and 2). So, comparison of free energies  $\Delta G_{298}$  (Table 3; figures in the parentheses) is probably more relevant than comparison of the total energies. In the tetracyclic drugs derived from artemisinin, the 1,2-dioxane compound, namely the 13-carbaartemisinin **7** and its 10-deoxy analogue **6**, are the more stable, with  $\Delta G(\text{T-S})_{298}$  values of 25.7 and 27.7 kcal mol<sup>-1</sup>, respectively. These values were significantly higher than the value obtained for the 1,2,4-trioxane parent drug artemisinin **1** (22.8 kcal mol<sup>-1</sup>). The computed stability of bicyclic 1,2-dioxanes **4m** and **5** is slightly lower as that of **6** and **7**, with  $\Delta G(\text{T-S})_{298}$  values of 23.7 and 24.9 kcal mol<sup>-1</sup> for **4m** and **5**, respectively, but still higher than that of artemisinin or the 3-spiro-1,2,4-trioxane **2** (20.8 kcal mol<sup>-1</sup>). Two slightly different  $\Delta G(\text{T-S})_{298}$  values, 18.4 and 18.6 kcal mol<sup>-1</sup>, were obtained for the 1,2,4,5-tetraoxane **9m**, which contains two peroxide bonds. Optimized geometry of **9m** is indeed slightly deviated from the *C<sub>s</sub>* symmetry, and this feature may be the cause of two O–O bond strength values which differs of 0.2 kcal mol<sup>-1</sup>. The  $\Delta G(\text{T-S})_{298}$  values obtained for the 1,2,4,5-tetraoxane **9m** and 1,2,4-trioxolane **8m** were 18.4/18.6 and 17.6 kcal mol<sup>-1</sup>, respectively, much lower than the O–O bond energy of all the computed 1,2-dioxane or 1,2,4-trioxane based drugs. The values obtained for the 3-spiro-1,2,4-trioxanes *cis*-**3m** and *trans*-**3m** (26.7 and 27.0 kcal mol<sup>-1</sup>, respectively) are much higher than that of the

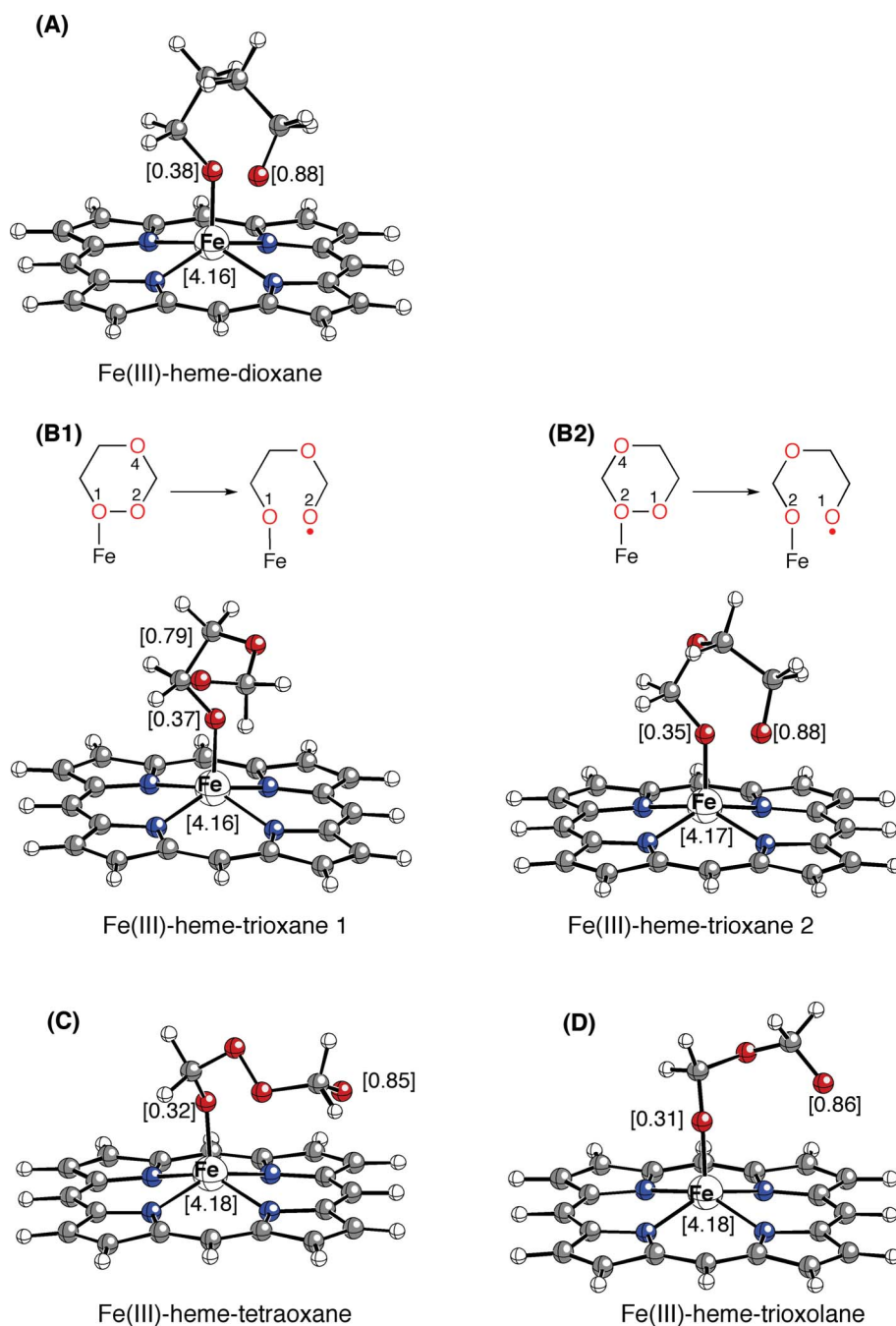
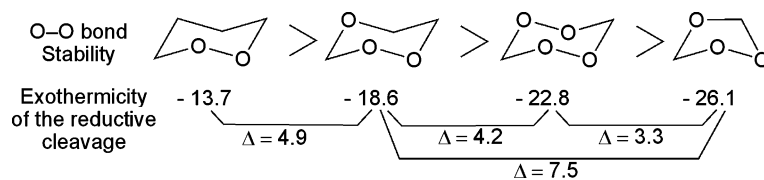


**Fig. 3** Fully optimized geometries (B3LYP/def2-SVP) of the complexes formed through the reductive cleavage of the naked cyclic peroxides by the model Fe<sup>II</sup>-heme complex. Computed spin densities are indicated in brackets.



**Scheme 3** Total gas-phase energies of the reductive cleavage of endoperoxides by high-spin iron(II)-heme [ $\Delta E$  (T-S), with ZPVE included, in kcal mol<sup>-1</sup>], computed at the B3LYP/6-31+G(d) level.

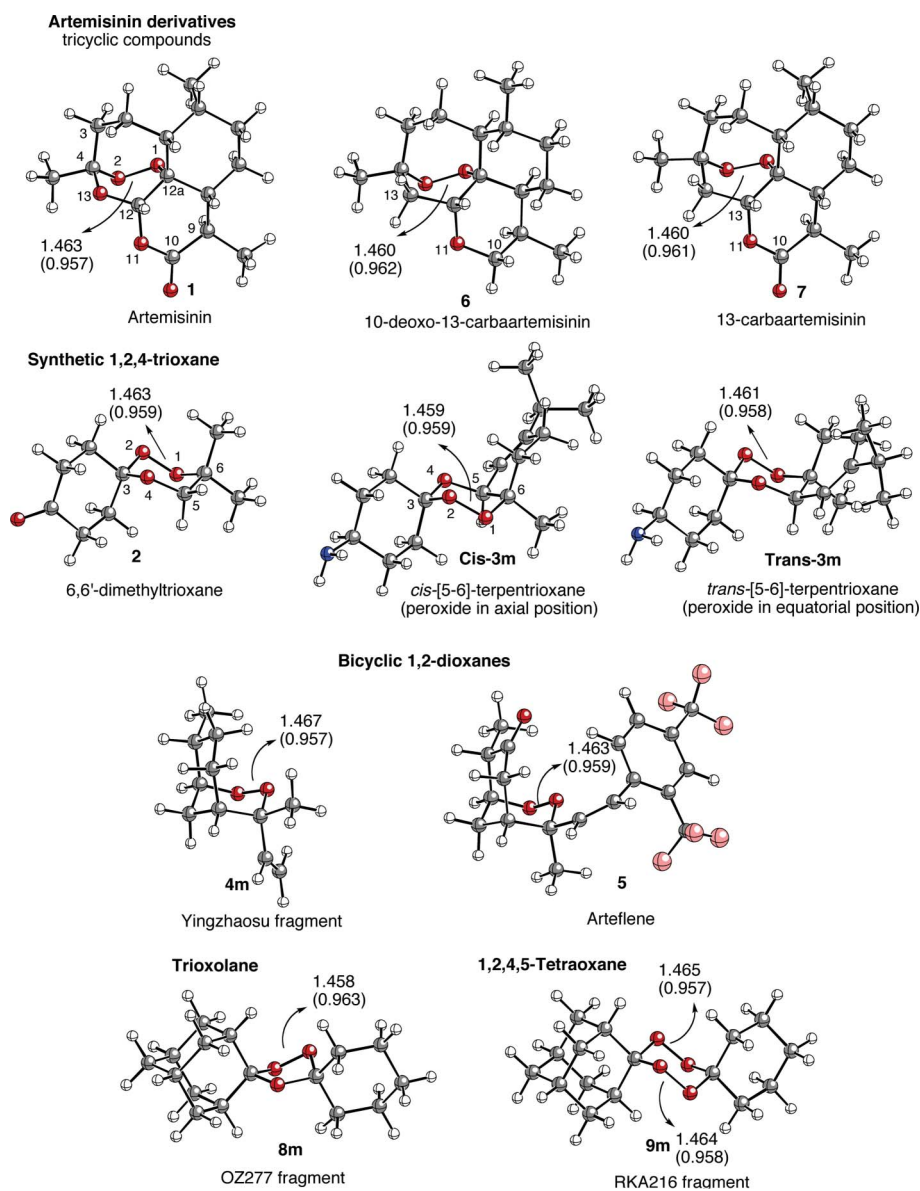


**Fig. 4** Ball & stick representations of 1–9 compounds. All structures correspond to fully optimized geometries at the B3LYP/6-31+G(d) level. O–O bond lengths are indicated in Å (plain figures), and corresponding NBO–Wiberg bond order values are in parentheses.

other 3-spiro-1,2,4-trioxanes **2** and comparable to the most stable 1,2-dioxane based drugs **6** and **7**. Compounds *cis*-**3m** and *trans*-**3m** have a 5,6-cyclohexene substituent, while **2** is less substituted with only dimethyl at position **6**. So, on the base of these computed energies, we can conclude that the decreasing stability of the peroxide bond follows the same trend found using the naked simplest cyclic peroxides order: 1,2-dioxane > 1,2,4-trioxane > 1,2,4,5-tetraoxane > 1,2,4-trioxolane for all compounds with the notable exception of *cis*-**3m** and *trans*-**3m**.

In addition, the computed bond orders and bond lengths showed in Fig. 4 are not a clear indication of the computed bond strength. This feature probably indicate that the O–O bond strength is also related to the whole structure of the drug, specially the substitution pattern of each drug and its cycle strain.

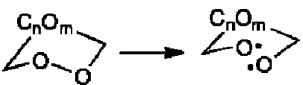
As the antibonding  $\sigma^*$  LUMO orbital of the peroxide bond has been considered to be involved in the reductive cleavage by

iron(II),<sup>26</sup> we were curious to compute the HOMO–LUMO gap for some representative antimalarial drugs (**1**, **7**, **8m** and **9m**). In all cases, both the HOMO and LUMO, which is clearly the antibonding  $\sigma^*$  orbital, are located in the O–O bond (Fig. 5 for drugs **1** and **8m**). Interestingly, the computed HOMO–LUMO gaps are: 6.63 eV (**1**), 6.25 eV (**7**), 6.83 eV (**8m**) and 6.69 eV (**9m**). This means that the 1,2-dioxane-based compound **7** exhibits the lowest HOMO–LUMO gap while the trioxolane **8m** presents the highest computed value. The trend given by the HOMO–LUMO gap is not exactly the same than that found using the exothermicity of the homolysis of the peroxide bond.

#### Correlation with antimalarial activity?

Beyond the comparison of O–O bond stabilities on a theoretical point of view, it should be interesting to correlate the O–O

**Table 3** Gas phase energy of the O–O bond in antimalarial drugs or models, computed at the B3LYP/6-31+G(d) level. Plain values indicate the total energies  $\Delta E$  (T-S), with ZPVE included. Values in parenthesis are the  $\Delta G_{298}$  free energies

Reaction 	IC <sub>50</sub> , relative potency <sup>b</sup>	$\Delta E$ (T-S) <sup>a</sup> ( $\Delta G_{298}$ ), kcal mol <sup>-1</sup>
1,2,4-trioxane, $n = m = 1$ <b>1</b> → <b>1(T)</b>	100	+ 24.5 (+ 22.8)
1,2-dioxane, $n = 2, m = 0$ <b>6</b> → <b>6(T)</b>	16 <sup>c</sup>	+ 29.4 (+ 27.7)
1,2-dioxane, $n = 2, m = 0$ <b>7</b> → <b>7(T)</b>	4 <sup>c</sup>	+ 28.1 (+ 25.7)
1,2,4-trioxane, $n = m = 1$ <b>2</b> → <b>2(T)</b>	nd	+ 23.5 (+ 20.8)
1,2,4-trioxane, $n = m = 1$ <i>cis</i> - <b>3m</b> → <i>cis</i> - <b>3m(T)</b>	[for <i>cis</i> - <b>3a</b> = 138 <sup>d</sup> ]	+ 28.8 (+ 26.7)
1,2,4-trioxane, $n = m = 1$ <i>trans</i> - <b>3m</b> → <i>trans</i> - <b>3m(T)</b>	[for <i>trans</i> - <b>3a</b> = 138 <sup>d</sup> ]	+ 29.0 (+ 27.0)
1,2-dioxane, $n = m = 1$ <b>4m</b> → <b>4m(T)</b>	nd	+ 25.7 (+ 23.7)
1,2-dioxane, $n = m = 1$ <b>5</b> → <b>5(T)</b>	18 <sup>e</sup>	+ 27.1 (+ 24.9)
1,2,4-trioxolane, $n = 0, m = 1$ <b>8m</b> → <b>8m(T)</b>	[for <b>8</b> = 407 <sup>f</sup> ]	+ 19.7 (+ 17.6)
1,2,4,5-tetraoxane, $n = 0, m = 2$ <b>9m</b> → <b>9m(T)</b>	[for <b>9</b> = 183 <sup>f</sup> ]	1st O–O bond: + 20.9 (+ 18.4) 2nd O–O bond: + 21.0 (+ 18.6)

<sup>a</sup> Triplet minus ground state energies (in kcal mol<sup>-1</sup>). <sup>b</sup> [IC<sub>50</sub> (**1**), nM/IC<sub>50</sub> (drug **N**), nM] × 100, evaluated on the chloroquine resistant W2-Indochina strain of *P. falciparum*, except where otherwise stated; nd = not determined. <sup>c</sup> Reference 9a. <sup>d</sup> On the chloroquine resistant FcM29-Cameroon strain, reference 8. <sup>e</sup> Reference 42. <sup>f</sup> Reference 16; activity evaluated on the chloroquine sensitive strain 3D7.

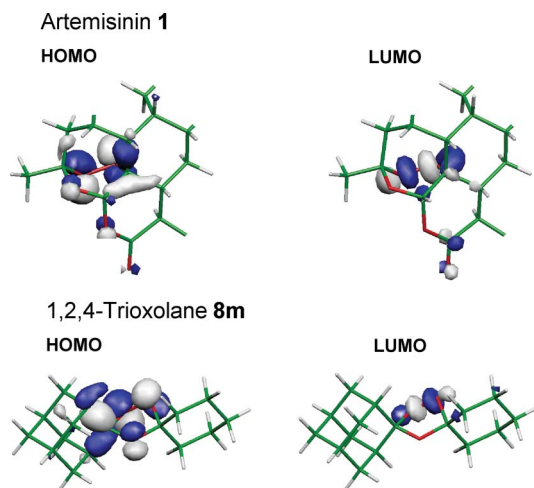


**Fig. 5** Frontier orbitals of compounds **1** and **8m** (isosurface value of 0.05 au).

bond energies of drugs with their antimalarial activity. The relative activity of drugs against a chloroquine resistant strain of *P. falciparum* is reported in Table 3, artemisinin being considered as reference (relative potency = 100). In the series of artemisinin derivatives, **1**, **6**, **7**, the more active drug artemisinin **1** has also the lower O–O bond homolysis exothermicity ( $\Delta G_{298} = 22.8$  kcal mol<sup>-1</sup>, relative potency = 100). However, the results obtained for **6** ( $\Delta G_{298} = 27.7$  kcal mol<sup>-1</sup>, relative potency = 16) and **7** ( $\Delta G_{298} = 25.7$  kcal mol<sup>-1</sup>, relative potency = 4) do not confirm a clear correlation between  $\Delta G_{298}$  and antimalarial activity. In

principle, such a correlation must be considered with care. Other factors than electronic status may indeed play a decisive role for biological activity. For instance, the steric hindrance in the vicinity of the peroxide may prevent the innersphere reduction of the O–O bond by iron(II)-heme.<sup>34,46</sup> In addition, some computed model structures indeed do not exactly fit with real drugs. More generally, correlation between O–O bond strength and activity cannot be applied to trioxaquinones *cis*-**3** and *trans*-**3** which are dual drugs, the quinoline fragment indeed being also necessary for antimalarial activity: *cis*-**3** and *trans*-**3** are much more active (IC<sub>50</sub> = 8 nM for both drugs) than their trioxane fragment **3** (see Fig. 4, IC<sub>50</sub> = 155 nM), despite similar O–O bond strengths are expected for **3**, *cis*-**3** and *trans*-**3**.

## Conclusion

The computational study reported herein clearly indicates that the thermal homolysis of several endoperoxide structures is well correlated with their reductive activation by iron(II)-heme. In 6-membered cycles, the more oxygen atoms in the cycle, the less stability, meaning that the stability order is the following: 1,2-dioxane > 1,2,4-trioxane > 1,2,4,5-tetraoxane. In cycles containing 3 oxygen atoms, the 5-membered cycle 1,2,4-trioxolane was found much less stable than its 6-membered counterpart trioxane. This feature indicates the possible role of the cycle strain for the O–O bond stability, and may also explain the high antimalarial activity of some trioxolane derivatives.

However, the O–O bond stability of endoperoxide drugs is not in itself a decisive argument to anticipate their antimalarial activity.



Other factors may be decisive for *in vivo* activity, among them (a) steric hindrance close to the O–O bond that may prevent the peroxide reduction by iron(II)-heme, (b) ability of the O' to produce C', and heme alkylation ability of this latter; for instance, arteflene is prone to react with Fe<sup>II</sup> but unable to alkylate a heme model,<sup>57</sup> (c) bioavailability and metabolism. In addition, correlation between O–O bond strength and biological activity cannot be considered for dual drugs, which have an additional biologically active moiety, such as trioxaquinones. Nevertheless, this approach can help to design thermally stable peroxide drugs. Beside biological activity, thermal stability is indeed an important issue for both convenient synthesis and easy storage of antimalarial drugs.

## Experimental Section

### Computational Details

All the calculations reported in this paper were obtained with the GAUSSIAN 03 suite of programs.<sup>47</sup> Electron correlation was partially taken into account using the hybrid functional usually denoted as B3LYP<sup>48–50</sup> and the standard triple or double- $\xi$  quality 6-311++G(d,p) and 6-31+G(d) basis sets.<sup>51</sup> For the calculations involving iron atoms, the double- $\xi$  plus polarization def2-SVP basis set for all atoms was used.<sup>52</sup> For model compounds, the MP2 method was also used.<sup>53</sup> Triplet and open-shell singlet species were computed at the unrestricted UB3LYP (or UMP2) level. Zero point vibrational energy (ZPVE) corrections were computed at the same level and were not scaled. Calculation of the vibrational frequencies<sup>54</sup> at the optimized geometries showed that the compounds are minima on the potential energy surface.

The Wiberg bond indices  $B_i$  and donor–acceptor interactions have been computed using the natural bond orbital (NBO) method.<sup>55–58</sup> The energies associated with these two-electron interactions have been computed according to the following equation:

$$\Delta E^{(2)} = -n_{\phi} \frac{\langle \phi^* | \hat{F} | \phi \rangle^2}{\varepsilon_{\phi^*} - \varepsilon_{\phi}}$$

where  $F$  is the DFT equivalent of the Fock operator and  $\phi$  and  $\phi^*$  are two filled and unfilled Natural Bond Orbitals having  $\varepsilon_{\phi}$  and  $\varepsilon_{\phi^*}$  energies respectively;  $n_{\phi}$  stands for the occupation number of the filled orbital.

Unless otherwise stated, Gibbs energies  $\Delta G$  have been computed at 298 K. Analytical Hessians were computed to calculate unscaled zero-point energies (ZPEs), as well as thermal corrections and entropy effects, using the standard statistical-mechanics relationships for an ideal gas.

### Antimalarial Activities

Due to the variability of laboratory strains of *Plasmodium*, in most cases, it is difficult to compare the IC<sub>50</sub> values reported in different studies: for instance IC<sub>50</sub> of artemisinin is 1.7 or 7.8 nM on W2.<sup>9a</sup> In addition, the activity is significantly different according to the *Plasmodium* strain used: IC<sub>50</sub> of artemisinin is 11 nM on FcM29 (both W2 and FcM29 are chloroquine-resistant). So, in this report, antimalarial activities extracted from bibliographic sources are given as relative potency with respect to artemisinin, which is used as control drug in all studies. So, the relative potency

of antimalarial drugs reported in Table 3 is calculated as  $[\text{IC}_{50}(\mathbf{1})/\text{IC}_{50}(\text{drug N})] \times 100$  for each drug N. IC<sub>50</sub> values were measured on W2-Indochina *P. falciparum*, except where otherwise stated.

## Acknowledgements

The authors gratefully acknowledge all co-authors of their articles on antimalarial drugs (artemisinin and trioxaquinones). AR is indebted to Dr Bernard MEUNIER for past and recent discussions on the stability of endoperoxides. CNRS provided financial support to the CNRS-LCC. IF thanks the Spanish MICINN and CAM (Grants CTQ2007-67528, Consolider-Ingenio 2010, CSD2007-00006, S2009/PPQ-1634, and Ramón y Cajal program) for financial support.

## References

- 1 D. L. Klayman, *Science*, 1985, **228**, 1049.
- 2 N. J. White, *Science*, 2008, **320**, 330.
- 3 S. R. Meshnick, T. E. Taylor and S. Kamchonwongpaisan, *Microbiol. Rev.*, 1996, **60**, 301.
- 4 N. J. White, F. Nosten, S. Looareesuwan, W. M. Watkins, K. Marsh, R. W. Snow, G. Kokwaro, J. Ouma, T. T. Hien, M. E. Molyneux, T. E. Taylor, C. I. Newbold, T. K. Ruebush, M. Danis, B. M. Greenwood, R. M. Anderson and P. Olliaro, *Lancet*, 1999, **353**, 1965.
- 5 F. Nosten and P. Brasseur, *Drugs*, 2002, **62**, 1315.
- 6 J. N. Cumming, P. Ploypradith and G. H. Posner, *Adv. Pharmacol.*, 1997, **37**, 253.
- 7 C. W. Jefford, *Adv. Drug Res.*, 1997, **29**, 271.
- 8 F. Bousejra-El Garah, J.-L. Stigliani, F. Coslédan, B. Meunier and A. Robert, *ChemMedChem*, 2009, **4**, 1469.
- 9 (a) M. A. Avery, F. Pingchen, J. M. Karle, J. D. Bonk, R. Miller and D. K. Goins, *J. Med. Chem.*, 1996, **39**, 1885; (b) M. Jung, X. Li, D. Bustos, H. ElSohly, J. McChesney and W. K. Milhous, *J. Med. Chem.*, 1990, **33**, 1516; (c) R. K. Haynes, B. Fugmann, J. Stetter, K. Rieckmann, H.-D. Heilmann, H.-W. Chan, M.-K. Cheung, W.-L. Lam, H.-N. Wong, S. L. Croft, L. Vivas, L. Rattray, L. Stewart, W. Peters, B. L. Robinson, M. D. Edstein, B. Kotecka, D. E. Kyle, B. Beckermann, M. Gerisch, M. Radtke, G. Schmuck, W. Steinke, U. Wollborn, K. Schmeer and A. Römer, *Angew. Chem., Int. Ed.*, 2006, **45**, 2082.
- 10 O. Dechy-Cabaret, F. Benoit-Vical, A. Robert and B. Meunier, *ChemBioChem*, 2000, 281.
- 11 O. Dechy-Cabaret, F. Benoit-Vical, C. Loup, A. Robert, H. Gornitzka, A. Bonhore, H. Vial, J. Magnaval, J. Séguéla and B. Meunier, *Chem.–Eur. J.*, 2004, **10**, 1625.
- 12 F. Coslédan, L. Fraisse, A. Pellet, F. Guillou, B. Mordmüller, P. G. Kremsner, A. Moreno, D. Mazier, J. P. Maffrand and B. Meunier, *Proc. Natl. Acad. Sci. U. S. A.*, 2008, **105**, 17579.
- 13 J. L. Vennerstrom, S. Arbe-Barnes, R. Brun, S. A. Charman, F. C. K. Chiu, J. Chollet, Y. Dong, A. Dorn, D. Hunziker, H. Matile, K. McIntosh, M. Padmanilayam, J. Santo Tomas, C. Scheurer, B. Scorneaux, Y. Tang, H. Urwyler, S. Wittlin and W. N. Charman, *Nature*, 2004, **430**, 900.
- 14 X. Wang, Y. Dong, S. Wittlin, D. Creek, J. Chollet, S. A. Charman, J. Santo Tomas, C. Scheurer, C. Snyder and J. L. Vennerstrom, *J. Med. Chem.*, 2007, **50**, 5840.
- 15 Y. Dong, S. Wittlin, K. Sriraghavan, J. Chollet, S. A. Charman, W. N. Charman, C. Scheurer, H. Urwyler, J. Santo Tomas, C. Snyder, D. J. Creek, J. Morizzi, M. Koltun, H. Matile, X. Wang, M. Padmanilayam, Y. Tang, A. Dorn, R. Brun and J. L. Vennerstrom, *J. Med. Chem.*, 2010, **53**, 481.
- 16 R. Amewu, A. V. Stachulski, S. A. Ward, N. G. Berry, P. G. Bray, J. Davies, G. Labat, L. Vivas and P. M. O'Neill, *Org. Biomol. Chem.*, 2006, **4**, 4431.
- 17 G. L. Ellis, R. Amewu, S. Sabbani, P. A. Stocks, A. Shone, D. Stanford, P. Gibbons, J. Davies, L. Vivas, S. Charnaud, E. Bongard, C. Hall, K. Rimmer, S. Lozanom, M. Jesús, D. Gargallo, S. A. Ward and P. M. O'Neill, *J. Med. Chem.*, 2008, **51**, 2170.
- 18 (a) P. M. O'Neill, R. K. Amewu, G. L. Nixon, F. Bousejra ElGarah, M. Mungthin, J. Chadwick, A. E. Shone, L. Vivas, H. Lander, V. Barton,

- S. Muangnoicharoen, P. G. Bray, J. Davies, B. K. Park, S. Wittlin, R. Brun, M. Preschel, K. Zhang and S. A. Ward, *Angew. Chem., Int. Ed.*, 2010, **49**, 5693; (b) Supporting Information of ref. 18a.
- 19 I. Eto, M. Akiyoshi, T. Matsunaga, A. Miyake and T. Ogawa, *J. Therm. Anal. Calorim.*, 2006, **85**, 623.
- 20 F. O. Rice and O. M. Reiff, *J. Phys. Chem.*, 1927, **31**, 1352.
- 21 A. J. Lin, D. L. Klayman and J. M. Hoch, *J. Org. Chem.*, 1985, **50**, 4504.
- 22 S. A.-L. Laurent, J. Boissier, F. Coslédan, H. Gornitzka, A. Robert and B. Meunier, *Eur. J. Org. Chem.*, 2008, 895.
- 23 G. H. Posner, C. H. Oh, D. Wang, L. Gerena, W. K. Milhous, S. R. Meshnick and W. Asawamahesakda, *J. Med. Chem.*, 1994, **37**, 1256.
- 24 A. Robert and B. Meunier, *Chem.–Eur. J.*, 1998, **4**, 1287.
- 25 A. Robert, J. Cazelles and B. Meunier, *Angew. Chem., Int. Ed.*, 2001, **40**, 1954.
- 26 A. Robert, O. Dechy-Cabaret, J. Cazelles and B. Meunier, *Acc. Chem. Res.*, 2002, **35**, 167.
- 27 S. A.-L. Laurent, A. Robert and B. Meunier, *Angew. Chem., Int. Ed.*, 2005, **44**, 2060.
- 28 A. Robert and B. Meunier, *Chem.–Eur. J.*, 1998, **4**, 1287.
- 29 M. Rodríguez, D. Delpon-Bonnet, J.-P. Bégué, A. Robert and B. Meunier, *Bioorg. Med. Chem. Lett.*, 2003, **13**, 1059.
- 30 F. Bousejra-El Garah, B. Meunier and A. Robert, *Eur. J. Inorg. Chem.*, 2008, 2133.
- 31 S. A.-L. Laurent, C. Loup, S. Mourgues, A. Robert and B. Meunier, *ChemBioChem*, 2005, **6**, 653.
- 32 J. Cazelles, A. Robert and B. Meunier, *J. Org. Chem.*, 2002, **67**, 609.
- 33 D. J. Creek, W. N. Charman, F. C. K. Chiu, R. J. Pranker, Y. Dong, J. L. Vennerstrom and S. A. Charman, *Antimicrob. Agents Chemother.*, 2008, **52**, 1291.
- 34 (a) F. Coslédan, L. Fraise, A. Pellet, F. Guillou, B. Mordmüller, P. G. Kremsner, A. Moreno, D. Mazier, J.-P. Maffrand and B. Meunier, *Proc. Natl. Acad. Sci. U. S. A.*, 2008, **105**, 17579; (b) P. M. O'Neill, R. K. Amewu, G. L. Nixon, F. Bousejra ElGarah, M. Mungthin, J. Chadwick, A. E. Shone, L. Vivas, H. Lander, V. Barton, S. Muangnoicharoen, P. G. Bray, J. Davies, B. K. Park, S. Wittlin, R. Brun, M. Preschel, K. Zhang and S. A. Ward, *Angew. Chem., Int. Ed.*, 2010, **49**, 5693.
- 35 A. Robert, F. Benoit-Vical, C. Claparols and B. Meunier, *Proc. Natl. Acad. Sci. U. S. A.*, 2005, **102**, 13676.
- 36 F. Bousejra-El Garah, C. Claparols, F. Benoit-Vical, B. Meunier and A. Robert, *Antimicrob. Agents Chemother.*, 2008, **52**, 2966.
- 37 H. Goff and G. N. La Mar, *J. Am. Chem. Soc.*, 1977, **99**, 6599.
- 38 B. Meunier and A. Robert, *Acc. Chem. Res.*, 2010, **43**, 1444.
- 39 C. Lacaze-Dufaure, F. Najjar and C. André-Barrès, *J. Phys. Chem. B*, 2010, **114**, 9848.
- 40 W. Nosoongnoen, J. Pratuangdejkul, K. Sathirakul, A. Jacob, M. Conti, S. Loric, J.-M. Launay and P. Manivet, *Phys. Chem. Chem. Phys.*, 2008, **10**, 5083.
- 41 A. M. Szpilman, E. E. Korshin, H. Rozenberg and M. D. Bachi, *J. Org. Chem.*, 2005, **70**, 3618.
- 42 C. Jaquet, H. R. Stohler, J. Chollet and W. Peters, *Trop. Med. Parasitol.*, 1994, **45**, 266.
- 43 For geometry optimizations, the following X-ray crystal structures from the CCDC were used: (i) artemisinin 1;<sup>44</sup> (ii) X-ray structure of 10-deoxy-13-carbaartemisinin<sup>9a</sup> 6 was used for minimization of 6 and 7; (iii) X-ray structure of yingzhaosu 4<sup>41</sup> was used for minimization of 4 m (iv) X-ray of artefene 5;<sup>42</sup> (v) X-ray structure of trioxanes 2;<sup>11</sup> X-ray structure of trioxaquinones Cis-3 and Trans-3<sup>11</sup> for trioxanes Cis-3m and Trans-3m; (vi) trioxolane 8<sup>45</sup> for the fragment 8 m, and (vii) tetraoxane 9<sup>16</sup> for the fragment 9m.
- 44 K.-L. Chan, K.-H. Yuen, H. Takayanagi, S. Janadasa and K.-K. Peh, *Phytochemistry*, 1997, **46**, 1209.
- 45 Y. Tang, Y. Dong, J. M. Karle, C. A. DiTusa and J. L. Vennerstrom, *J. Org. Chem.*, 2004, **69**, 6470.
- 46 J. Cazelles, A. Robert and B. Meunier, *J. Org. Chem.*, 1999, **64**, 6776.
- 47 *Gaussian 03, Revision D.01*, M. J. Frisch, G. W. Trucks, H. B. Schlegel, G. E. Scuseria, M. A. Robb, J. R. Cheeseman, J. A. Montgomery, Jr., T. Vreven, K. N. Kudin, J. C. Burant, J. M. Millam, S. S. Iyengar, J. Tomasi, V. Barone, B. Mennucci, M. Cossi, G. Scalmani, N. Rega, G. A. Petersson, H. Nakatsuji, M. Hada, M. Ehara, K. Toyota, R. Fukuda, J. Hasegawa, M. Ishida, T. Nakajima, Y. Honda, O. Kitao, H. Nakai, M. Klene, X. Li, J. E. Knox, H. P. Hratchian, J. B. Cross, V. Bakken, C. Adamo, J. Jaramillo, R. Gomperts, R. E. Stratmann, O. Yazyev, A. J. Austin, R. Cammi, C. Pomelli, J. W. Ochterski, P. Y. Ayala, K. Morokuma, G. A. Voth, P. Salvador, J. J. Dannenberg, V. G. Zakrzewski, S. Dapprich, A. D. Daniels, M. C. Strain, O. Farkas, D. K. Malick, A. D. Rabuck, K. Raghavachari, J. B. Foresman, J. V. Ortiz, Q. Cui, A. G. Baboul, S. Clifford, J. Cioslowski, B. B. Stefanov, G. Liu, A. Liashenko, P. Piskorz, I. Komaromi, R. L. Martin, D. J. Fox, T. Keith, M. A. Al-Laham, C. Y. Peng, A. Nanayakkara, M. Challacombe, P. M. W. Gill, B. Johnson, W. Chen, M. W. Wong, C. Gonzalez, and J. A. Pople, Gaussian, Inc., Wallingford CT, 2004.
- 48 A. D. Becke, *J. Chem. Phys.*, 1993, **98**, 5648.
- 49 C. Lee, W. Yang and R. G. Parr, *Phys. Rev. B*, 1988, **37**, 785.
- 50 S. H. Vosko, L. Wilk and M. Nusair, *Can. J. Phys.*, 1980, **58**, 1200.
- 51 W. J. Hehre, L. Radom, P. V. R. Schleyer, J. A. Pople, *Ab Initio Molecular Orbital Theory*, Wiley, New York, 1986, p. 76 and references therein.
- 52 F. Weigend and R. Ahlrichs, *Phys. Chem. Chem. Phys.*, 2005, **7**, 3297.
- 53 (a) C. Møller and M. S. Plesset, *Phys. Rev.*, 1934, **46**, 618; (b) M. Head-Gordon, J. A. Pople and M. J. Frisch, *Chem. Phys. Lett.*, 1988, **153**, 503; (c) M. J. Frisch, M. Head-Gordon and J. A. Pople, *Chem. Phys. Lett.*, 1990, **166**, 275.
- 54 J. W. McIver and A. K. Komornicki, *J. Am. Chem. Soc.*, 1972, **94**, 2625.
- 55 J. P. Foster and F. Weinhold, *J. Am. Chem. Soc.*, 1980, **102**, 7211.
- 56 A. E. Reed and F. Weinhold, *J. Chem. Phys.*, 1985, **83**, 1736.
- 57 A. E. Reed, R. B. Weinstock and F. Weinhold, *J. Chem. Phys.*, 1985, **83**, 735.
- 58 A. E. Reed, L. A. Curtiss and F. Weinhold, *Chem. Rev.*, 1988, **88**, 899.